Trans. JSASS Aerospace Tech. Japan
Vol. 10, No. ists28, pp. Pc_67-Pc_72, 2012

Original Paper

Enhancement of a Spring-mass System Model for Numerical Simulations of Centrifugal Deployment Dynamics of Folded Square Membranes

By Nobukatsu OKUIZUMI[1)], Azusa MUTA[2)] and Saburo MATUNAGA[1)]

[1)]*The Institute of Space and Astronautical Science, Japan Aerospace Exploration Agency, Sagamihara, Japan*
[2)]*Department of Mechanical and Aerospace Engineering, Graduate School of Tokyo Institute of Technology, Tokyo, Japan*

(Received June 27th, 2011)

In this paper, the spring-mass system model developed for simple numerical simulations of thin membranes is enhanced by taking into account the properties of buckling and creases. The model is applied to the numerical simulations of centrifugal deployments of folded square membranes that are small-scale models for solar sail spacecraft "IKAROS". First the folding and deployment methods are reviewed. Then the formulation of the enhanced spring-mass system model is explained. Numerical simulations of the centrifugal deployments of two kinds of folded square membranes with different crease intervals are performed and the numerical results are compared with the corresponding experimental results. The deployment behaviors are discussed and the validity of the spring-mass system model is examined.

Key Words: Membrane, Simulation, Spring-mass Model, Centrifugal Deployment, Solar Sail

Nomenclature

E	:	Young's modulus of membrane
ν	:	Poisson's ratio of membrane
ρ	:	density of membrane
h	:	thickness of membrane
S	:	area of a triangular element
L_i	:	side length of a triangular element
m_i	:	mass of a particle of a triangular element
k_i	:	spring constant of a triangular element
δ_{ij}	:	Kronecker delta
l_{cr}	:	buckling length of a spring
α	:	tuning parameter for buckling
β	:	tuning parameter for crease stiffness
γ	:	contact penalty factor
θ	:	angle of crease
θ_0	:	natural angle of crease
J	:	geometrical moment of area per unit width
ζ	:	damping ratio
D	:	air drag force acts on an element
ρ_{air}	:	density of air

1. Introduction

Deployable structures using membranes have been studied for the development of light-weight and large space structures. Especially, solar sails are attracting much attention in the US, Europe and Japan. In Japan, a solar power sail demonstration spacecraft "IKAROS" was developed by JAXA and was launched on May 21th, 2010 by H-IIA launch vehicle.[1,2)] Fig. 1 shows an overview of "IKAROS" in space. The square solar sail with 20 meters in diagonal and 7.5 micrometers in thickness was successfully deployed by centrifugal force using no extendable booms. The deployment of the sail consists of two stages. In the first stage, four folded membrane strips are quasistatically reeled out. In the second stage, the strips are dynamically unfurled to be the square sail. Since ground experiments of the dynamic deployment are not possible, small-scale experiments and numerical analysis are necessary. The authors have conducted dynamic deployment experiments of the 2nd stage with small scale membranes similar to the IKAROS membrane in a vacuum chamber[3)]. In this paper, a spring-mass system model, which is referred to as multi-particle model, is enhanced by taking account of the buckling, crease stiffness and the contact around creases to perform simulations of the deployment experiments. The numerical results are compared with the results of experiments to examine the validity of the simulations.

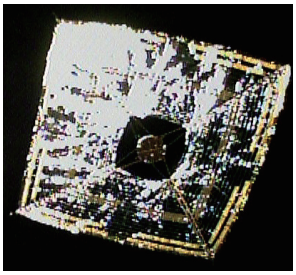

Fig. 1. Overview of "IKAROS".

2. Folding and Deployment Method

The folding method of the solar sail of "IKAROS" is illustrated in Fig. 2. The square membrane is composed of four trapezoidal petals. The petals are accordion-folded to become long strips. Then four strips are connected to be a cross-like shape. The center of the membrane is attached to the spacecraft with tethers and the strips are reeled up around the spacecraft. The deployment proceeds in two stages. In the first stage, the strips are quasistatically reeled out to return to the cross-like shape by relatively rotating four guide bars

Copyright© 2012 by the Japan Society for Aeronautical and Space Sciences and ISTS. All rights reserved.

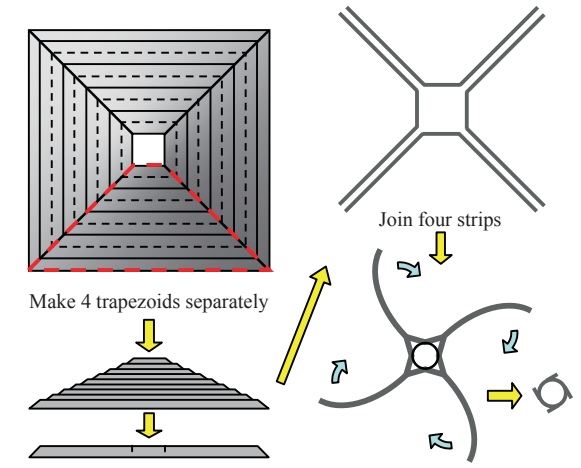

Fig. 2. Folding method.

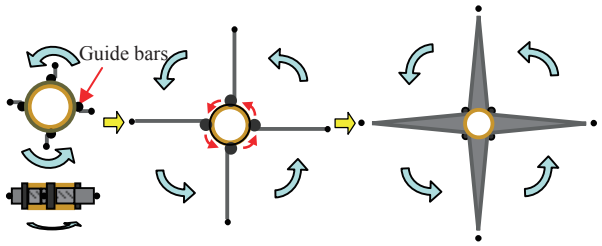

Fig. 3. First stage of deployment (quasistatic).

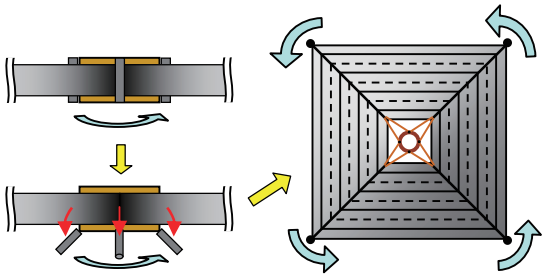

Fig. 4. Second stage of deployment (dynamic).

around the spacecraft as shown in Fig. 3. In the second stage, the guide bars are instantaneously turned down and the petals are deployed dynamically as shown in Fig. 4.

3. Spring-mass System Model

The spring-mass system model simulates in-plain elasticity of thin membranes by a network of springs and masses and has been developed for simple and fast numerical simulations of dynamic behaviors of the membranes. A rectangular element was first developed[4] to model square membranes and a triangular element shown in Fig. 5 was developed[5] to discretize the membranes with arbitrary shapes. The spring-mass system model using triangular elements was extended by taking account of buckling, crease stiffness to be applied to the centrifugal deployment of a hexagonal membrane with spiral folding and the validity was confirmed[6,7]. In this paper, the model is enhanced further to simulate the deployment behaviors of the folded square membranes.

3.1. Triangular element[5]

In Fig. 5, E, ρ, h and S represent Young's modulus, density, thickness and area of the membrane element, respectively and L_i (i=1,2,3) denote lengths of the sides of the triangle. The mass of the element ρhS is equally distributed to the lumped masses m_1, m_2 and m_3. The spring constants k_i are determined so that strain energy of the membrane and the potential energy of the springs coincide when the element is in one-axis stress states parallel to three sides and they are obtained by Eq. (1).

$$\begin{pmatrix} k_1 \\ k_2 \\ k_3 \end{pmatrix} = B_{ij}^{-1} \begin{pmatrix} 1 \\ 1 \\ 1 \end{pmatrix}, \quad B_{ij} = \frac{p_{ij}^2 L_i^2}{EhS}, \quad p_{ij} = 1 - \frac{4(1+\nu)S^2}{L_i^2 L_j^2}(1-\delta_{ij}), \tag{1}$$

where ν and δ_{ij} denote Poisson's ratio and Kronecker delta, respectively. Using this element, the models for buckling strength, crease stiffness, contact, damping and air drag are introduced as follows.

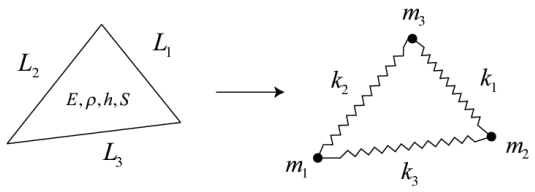

Fig. 5. Triangular element.

3.2. Buckling model

The restoring forces of the spring is assumed to become constant when the length of the spring is less than a critical value l_{cr} as shown in Fig. 6. The critical value l_{cr} is expressed using Euler buckling strength of a slender column as:

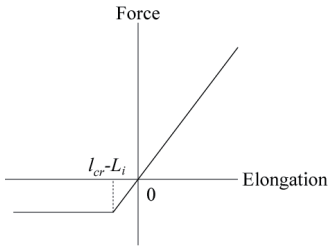

Fig. 6. Spring force.

$$l_{cr} = L_i - \alpha \frac{\pi^2 h^2}{12 L_i}, \tag{2}$$

where α is a parameter to adjust the buckling strength to actual membranes.

3.3. Crease stiffness and contact

Two triangular elements ABC and ABD that contain a crease are considered as shown in Fig. 7. It is assumed that the crease generates restoring forces F_C and F_D on masses C and D according to the difference between angle θ and natural crease angle θ_0. F_C and F_D are assumed to be orthogonal to the triangles and described as:

$$F_C = \beta \bar{\gamma} \frac{EJl_{AB}(\theta - \theta_0)}{l_{CE}^2}, \quad F_D = \beta \bar{\gamma} \frac{EJl_{AB}(\theta - \theta_0)}{l_{DF}^2},$$

$$\bar{\gamma} = \begin{cases} 1 & \text{when } \theta \geq 0 \\ \gamma & \text{when } \theta < 0 \end{cases}, \tag{3}$$

where $J=h^3/12$ denotes geometrical moment of area per unit width. γ represents a penalty factor to take account of self contacts around the crease lines. F_A and F_B are concentrated forces acting on the masses A and B to cancel rigid-body motion of the triangular elements and described as:

$$\mathbf{F}_A = -\frac{l_{BE}}{l_{AB}}\mathbf{F}_C - \frac{l_{BF}}{l_{AB}}\mathbf{F}_D,\ \mathbf{F}_B = -\frac{l_{AE}}{l_{AB}}\mathbf{F}_C - \frac{l_{AF}}{l_{AB}}\mathbf{F}_D. \quad (4)$$

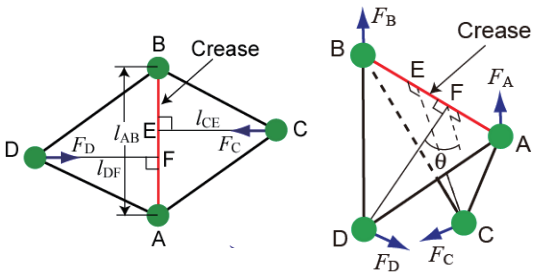

Fig. 7. Forces around crease.

3.4. Damping and air drag

Velocity-proportional dampers are added parallel to the springs to take account of structural damping. The damping coefficient is described as $2\zeta\sqrt{k_i m}$, where ζ denotes damping ratio and $m=(m_j+m_k)/2$. The air drag force due to the residual air in the vacuum chamber which acts on an element is distributed to three masses. The force applied to a mass is approximated as

$$D = \frac{1}{6}\rho_{\text{air}} S_n V^2, \quad (5)$$

where ρ_{air}, V and S_n denote air density, the velocity of the mass and the area of element projected to the direction of the velocity, respectively.

3.5 Equation of motion

The equations of motion of the system are described using rotating cylindrical coordinate system as

$$m\frac{d^2}{dt^2}(r,\theta,z)^T = \left(F_r + r\dot{\theta}^2, F_\theta - 2\dot{r}\dot{\theta}, F_z\right)^T, \quad (5)$$

where F_r, F_θ and F_z denote forces applied to the mass by the springs and creases, damping and air drag. These equations are numerically integrated by the Runge-Kutta method.

4. Numerical Results

4.1. Numerical model

Numerical simulations of the centrifugal deployment experiments are performed employing the spring-mass system model. Two models with different crease intervals are considered. The dimensions and material property of them are given in Table 1. Tip masses ace connected to four corners. Overviews of the numerical models 1 and 2 are shown in Figs. 8 and 9, respectively. Simulation parameters used here are listed in Table 2. Both models have the same segmentation. Triangular elements are arranged along folding lines. The tethers are modeled by springs and masses. The contact between tethers and central spool is taken into account. The natural crease angle is set to zero for simplicity. The experimental models were creased hard and the angles are small but vary. The buckling parameter of springs which are

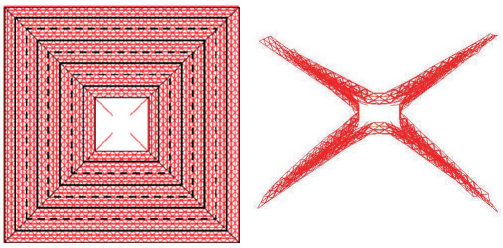

(a) Deployed (b) Before deployment

Fig. 8. Numerical model 1.

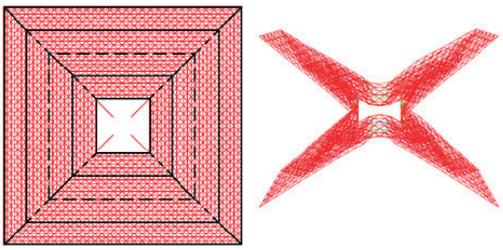

(a) Deployed (b) Before deployment

Fig. 9. Numerical model 2.

Table 1. Properties of the models.

Model No.	1	2
Number of folding lines	7	3
Outer width	455 mm	
Inner width	103 mm	
Thickness	7.5 μm	
Inner radius of stowed shape	25 mm	
Crease interval	22 mm	44 mm
Young's modulus of membrane	3.2 GPa	
Poisson's ratio of membrane	0.34	
Density of membrane	1420 kg/m^3	
Tether length	47.8 mm	
Weight of tip masses	0.36 g	

Table 2. Simulation parameters.

Number of masses	1980
Number of springs	5432
Number of elements	3456
Natural crease angle	0 rad
Buckling parameter α	100
Buckling parameter α on creases	1000
Crease stiffness parameter β	10
Contact penalty factor γ	100
Damping ratio	0.02
Rotation speed	3 Hz
Air pressure in chamber	4.5 Pa

not on creases is assumed to be 100 in accordance with the previous analysis for different folding method[6,7] and other tuning parameters α on creases, β and γ were searched by trial and error. In this paper, examples of numerical results with one combination of the tuning parameters are illustrated.

4.2. Numerical results

Fig. 10 shows an example of membrane shapes obtained by the numerical simulations of model 1. Membrane shapes during the deployment are computed using the rotating coordinate system. Snapshots of the experimental model 1 during the deployment taken by a spatially fixed camera are shown in Fig. 11. The numerical simulation captures the characteristics of the deployment behavior. The in-plane

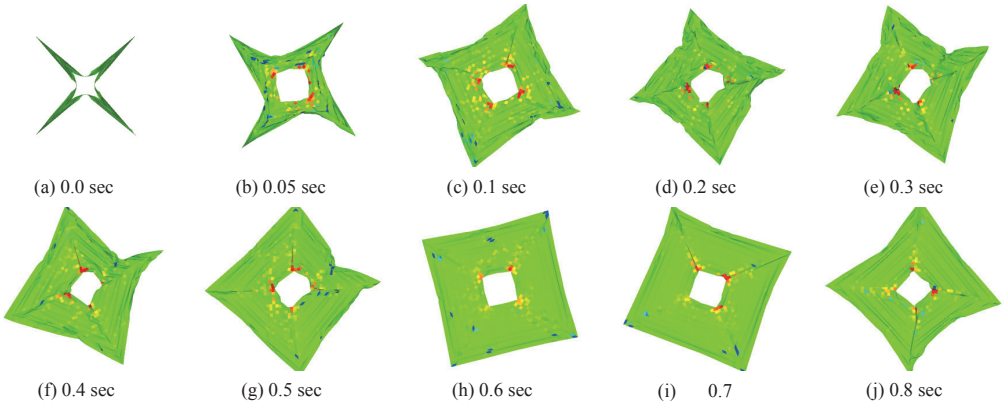

Fig. 10. Membrane shapes of numerical model 1 during deployment (α=1000 on creases, β=10, γ=100).

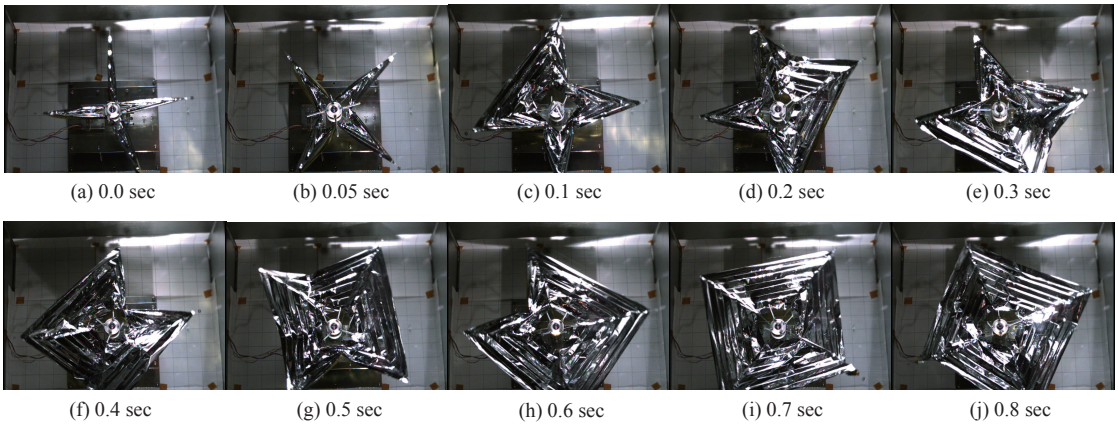

Fig. 11. Membrane shapes of experimental model 1 during deployment.

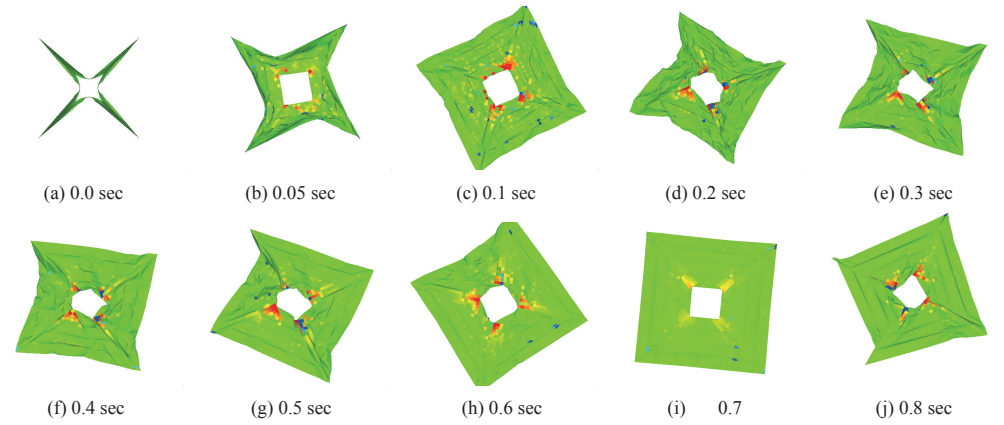

Fig. 12. Membrane shapes of numerical model 2 during deployment (α=1000 on creases, β=10, γ=100).

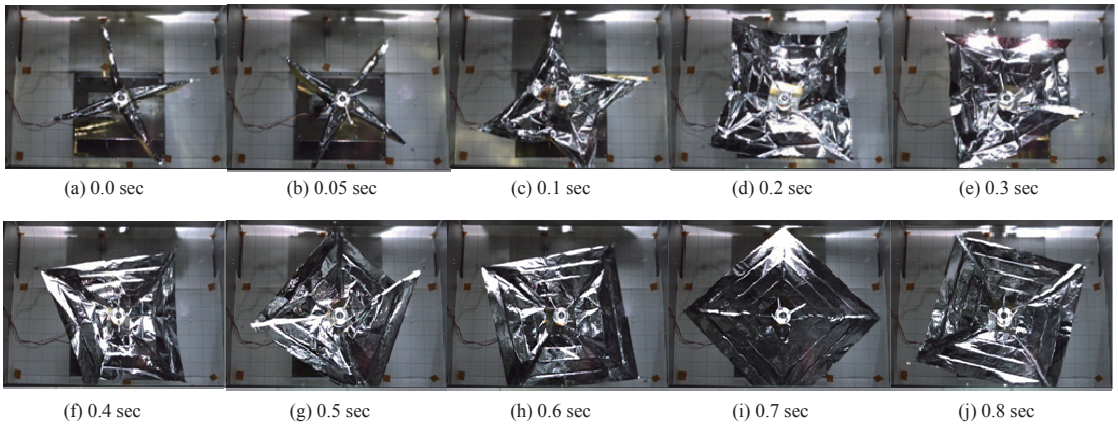

Fig. 13. Membrane shapes of experimental model 2 during deployment.

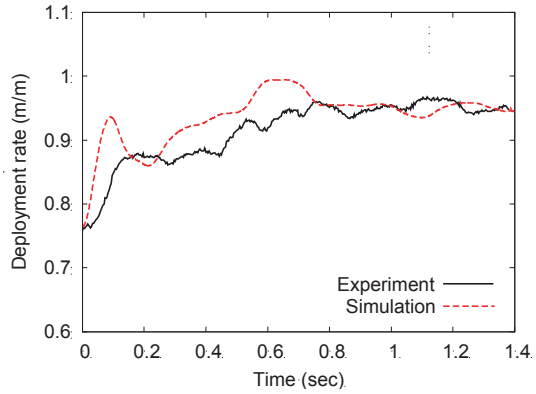

Fig. 14. Comparison of deployment rate (Model 1).

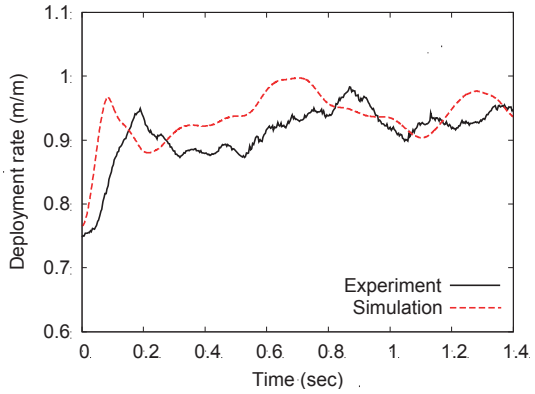

Fig. 15. Comparison of deployment rate (Model 2).

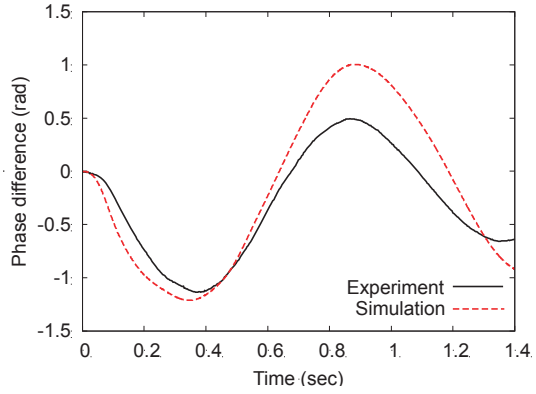

Fig. 16. Comparison of phase difference (Model 1).

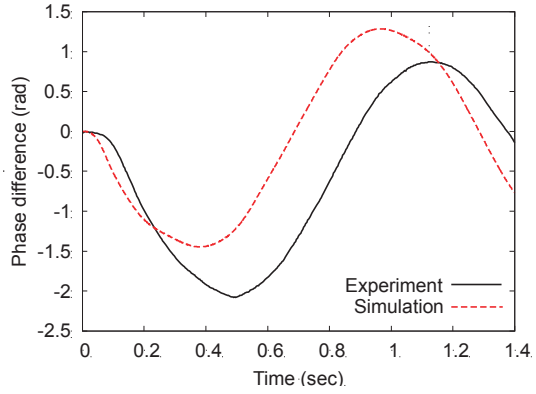

Fig. 17. Comparison of phase difference (Model 2).

vibration, asymmetric deformations and folding lines observed in the experiment appear in the simulation although the asymmetric flexures are not so sharp as the experimental model. Figs. 12 and 13 shows the same comparison in the case of model 2. The numerical result is also qualitatively similar to experimental result. The membrane shapes during deployment are also asymmetric but the behavior is smoother than model 1 because the effect of creases are reduced.

Figs. 14-17 show the quantitative comparison of the numerical and experimental results. It is noted that the quantitative repeatability of the experiments is not high so that the accurate comparison between the experiments and the simulations is not adequate. Figs. 14 and 15 show the time histories of deployment rates in model 1 and 2, respectively. The deployment rate is the ratio of the averaged radius of four corners during deployment normalized by the radius of pristine membrane. In model 1, the radius of the numerical result during deployment is larger than the experimental result. This is probably because the buckling strength of the experimental model is slightly higher than the numerical model. On the other hand, in model 2, the deployment rates of both results are quite similar except that the increase of the deployment rate in the experiments starts late.

Figs. 16 and 17 display the phase differences between the membrane and the central spool for model 1 and 2, respectively. The phase difference is the average of rotation angles ϕ of four corners relative to the spool as shown in Fig. 18. Figs. 16 and 17 clearly demonstrate the in-plain vibrations of the membranes. In model 1, the initial amplitudes of the experiment and simulation almost coincide with the each other although the damping of the experimental model is larger. In model 2, the initial amplitude of the simulation is smaller and the damping of the experimental model is also larger. The period of the vibration is larger than model 1 because model 2 with less folding lines is flexible than model 1. It is noted that the membrane reaches full deployment when the phase difference becomes zero in both the experiment and the simulations.

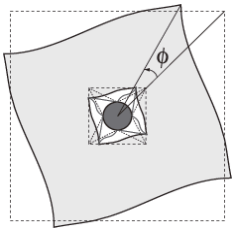

Fig. 18. Phase difference.

Since the values of the tuning parameters are the same in model 1 and 2, the above results can be improved by tuning the parameter values in accordance with the crease intervals.

5. Conclusions

The validity of the spring-mass system model is demonstrated by conducting the simulations of centrifugal deployments of small accordion-folded square membranes. In the case of large membrane space structures like “IKAROS”, the ratio of thickness to the width is extremely small. The investigations of physical bases of the models for buckling and creases will be necessary to improve the accuracy and to find the method to determine the tuning parameter values for membranes with various dimensions. Detailed analysis of the on-orbit deployment behavior of “IKAROS” and the improvement of the accuracy of the small-scale deployment experiments are currently in progress[8]. Through these studies, the spring-mass system model will be a practical tool for the developments of membrane structures.

References

1) Mori, O., et.al: World's First Demonstration of Solar Power Sailing by IKAROS, The Second International Symposium on Solar Sailing, New York, NY, 2010.
2) Sawada, T., et.al: Mission Report on The Solar Power Sail Deployment Demonstration of IKAROS, The 12th AIAA Gossamer systems forum, Denver, CO, USA, AIAA-2011-1887, 2011.
3) Muta, A, Matsunaga, S. and Okuizumi, N.: High Vacuum Experiment of Spinning Deployment Using Scaled-down Model For Solar Sail, International Astronautical Congress, IAC-10-C2.5.4, Prague, Czech, 2010.
4) Natori, M.C., Nakamura, F. and Okuizumi, N.: "Particle System Approximation for Dynamic Behavior of Membranes", International Symposium on Space Technology and Science, 2006-c-11, Kanazawa, Japan, 2006.
5) Miyazaki, Y. and Iwai, Y.: Dynamics of Membrane Deployed by Centrifugal Force, Space Engineering Conference, Tokyo, Japan,2005, pp.59-64 (in Japanese).
6) Okuizumi, N., and Yamamoto, T.: Centrifugal Deployment of Membrane with Spiral Folding: Experiment and Simulation, Journal of Space Engineering, **2** (2009), pp.41-50.
7) Okuizumi, N: "Deployment Dynamics of Membranes with Spiral Folding by Centrifugal Force", 11th AIAA Gossamer systems forum, 50th AIAA/ASME/ASCE/AHS/ASC Structures, Structural Dynamics, and Materials Conference, Orlando, FL, AIAA-2010-2583, 2010.
8) Shirasawa, Y., et.al: "Analysis of Membrane Dynamics using Multi-Particle Model for Solar Sail Demonstrator "IKAROS", 12th AIAA Gossamer systems forum, 52nd AIAA/ASME/ASCE/AHS/ASC Structures, Structural Dynamics, and Materials Conference, Denver, CO, AIAA-2011-1890, 2011.